# Melatonin-mediated upregulation of Sirt3 attenuates sodium fluoride-induced hepatotoxicity by activating the MT1-PI3K/AKT-PGC-1α signaling pathway

Chao Song, Jiamin Zhao, Beibei Fu, Dan Li, Tingchao Mao, Wei Peng, Haibo Wu, Yong Zhang

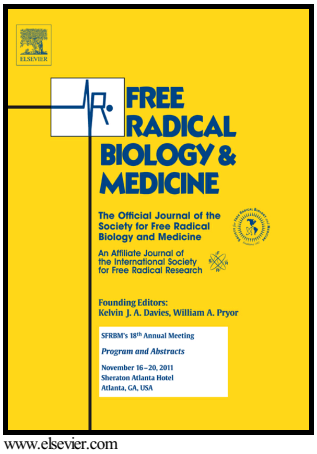


www.elsevier.com

PII: S0891-5849(17)30749-9
DOI: http://dx.doi.org/10.1016/j.freeradbiomed.2017.09.005
Reference: FRB13443

To appear in: *Free Radical Biology and Medicine*

Received date: 23 April 2017
Revised date: 28 August 2017
Accepted date: 8 September 2017

Cite this article as: Chao Song, Jiamin Zhao, Beibei Fu, Dan Li, Tingchao Mao, Wei Peng, Haibo Wu and Yong Zhang, Melatonin-mediated upregulation of Sirt3 attenuates sodium fluoride-induced hepatotoxicity by activating the MT1-PI3K/AKT-PGC-1α signaling pathway, *Free Radical Biology and Medicine,* http://dx.doi.org/10.1016/j.freeradbiomed.2017.09.005

**Running head of the title:** Melatonin alleviates NaF-induced hepatotoxicity

**Title:** Melatonin-mediated upregulation of Sirt3 attenuates sodium fluoride-induced hepatotoxicity by activating the MT1-PI3K/AKT-PGC-1α signaling pathway

**Authors:** Chao Song[a, b, 1], Jiamin Zhao[a, b, 1], Beibei Fu[a, b], Dan Li[a, b], Tingchao Mao[a, b], Wei Peng[a, b, 1], Haibo Wu[a, b,*], Yong Zhang[a, b,*]

**Author affiliations:** [a] College of Veterinary Medicine, Northwest A&F University, Yangling 712100, Shaanxi, China.

[b] Key Laboratory of Animal Biotechnology, Ministry of Agriculture, Northwest A&F University, Yangling 712100, Shaanxi, China.

[1] These authors contributed equally to this study.

**Corresponding author:** *Correspondence should be addressed to Haibo Wu or Yong Zhang.

Tel.: +86 29 87080092

Fax: +86 29 87080092

E-mail: hbwu029@nwsuaf.edu.cn (H.W) or zhangy1956@sina.com (Y.Z)

**Abstract**

Mitochondrial reactive oxygen species (ROS) production has been implicated in the pathogenesis of fluoride toxicity in liver. Melatonin, an indolamine synthesized in the pineal gland, was previously shown to protect against sodium fluoride (NaF)-induced hepatotoxicity. This study investigated the protective effects of melatonin pretreatment on NaF-induced hepatotoxicity and elucidates the potential mechanism of melatonin-mediated protection. Reducing mitochondrial ROS by melatonin substantially attenuated NaF-induced NADPH oxidase 4 (Nox4) upregulation and cytotoxicity in L-02 cells. Melatonin exerted its hepatoprotective effects by upregulating Sirtuin 3 (Sirt3) expression level and its activity. Melatonin increased the activity of manganese superoxide dismutase (SOD2) by promoting Sirt3-mediated deacetylation and promoted SOD2 expression through Sirt3-regulated DNA-binding activity of forkhead box O3 (FoxO3a), thus inhibiting the production of mitochondrial ROS induced by NaF. Notably, increased peroxisome proliferator-activated receptor gamma coactivator 1α (PGC-1α) by melatonin activated the Sirt3 expression, which was regulated by an estrogen-related receptor (ERR) binding element (ERRE) mapped to Sirt3 promoter region. Analysis of the cell signaling pathway profiling systems and specific pathway inhibition indicated that melatonin enhances PGC-1α expression by

activating the PI3K/AKT signaling pathway. Importantly, inhibition of melatonin receptor (MT)-1 blocked the melatonin-activated PI3K/AKT-PGC-1α-Sirt3 signaling. Mechanistic study revealed that the protective effects of melatonin were associated with down-regulation of JNK1/2 phosphorylation. Our findings provided a theoretical basis that melatonin mitigated NaF-induced hepatotoxicity, which, in part, was mediated through the activation of the Sirt3 pathway.



Graphical abstract

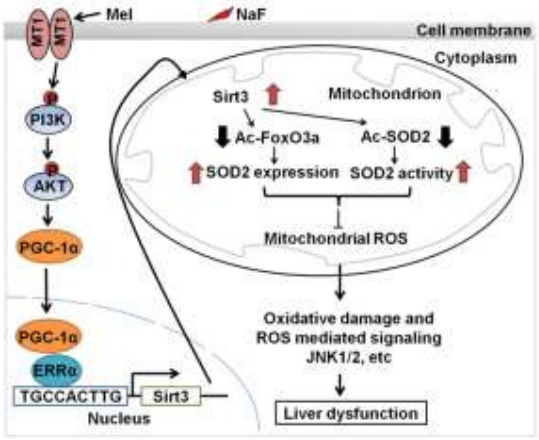


**Keywords:** Melatonin; Sodium fluoride; Hepatotoxicity; SIRT3; SOD2; PI3K/AKT

## [1]Introduction

Fluorosis, a progressive degenerative disorder caused by excessive fluoride intake either by anthropogenic or by natural sources and most commonly via drinking water [1]. Endemic fluorosis is now known to be global in scope, occurring in many parts of the world and affecting millions of people [2]. Fluorosis causes damage not only to teeth and skeletal tissue but also soft tissues including liver [3-5]. Liver is

---

[1] **Abbreviations:** NaF, Sodium; ROS, Reactive oxygen species; $O_2^{\bullet-}$ ,superoxide; GSH, Glutathione; MDA, Malondialdehyde; Bax, Bcl2-associated X protein; Bcl-2, B-cell CLL/lymphoma 2; GAPDH, Glyceraldehyde-3-Phosphate Dehydrogenase; COXIV, Cytochrome C Oxidase Subunit IV; Nox4, NADPH Oxidase 4; Sirt3, Sirtuin 3; SOD2, Manganese superoxide dismutase; FoxO3a, Forkhead box O3; AMPK, Adenosine monophosphate-activated protein kinase; PGC-1α, Peroxisome proliferator-activated receptor gamma coactivator 1α; NRF1, nuclear respiratory factor 1; ERRα, Estrogen-related receptor alpha; DLR, Dual luciferase reporter; ChIP, Chromatin immunoprecipitation assay; EMSA, Electrophoretic mobility shift assay; AKT, RAC-alpha serine/threonine-protein kinase; JNK1, c-Jun N-terminal kinase 1; p53, Tumor suppressor p53; ALT, Alanine aminotransferase; AST, Aspartate aminotransferase; MAPKs, Mitogen-activated protein kinases; MT1, Melatonin Receptor 1A; MT2, Melatonin Receptor 1B.

one of the vital organs susceptible to fluoride toxicity [6], plethora of studies suggest that fluoride causes hepatic dysfunction through free radicals mediated oxidative stress [7], mitochondrial dysfunction [8], and apoptotic cell death [9]. Oxidative stress, which can be defined as an imbalance between the presence of antioxidant enzymes and the production of reactive oxygen species (ROS), is considered to play an important role in the toxic effects of fluoride [10, 11]. Mitochondria are the main producers of ROS and are believed to be a primary target for NaF-induced hepatotoxicity [6, 12, 13]. Moreover, accumulating lines of evidence suggest that NADPH oxidases participate in the production of ROS generated by fluoride treatment [14, 15]. Recent studies have reported that Nox4 predominantly exists in the mitochondria in liver [16] and fluoride exposure induced Nox4 expression in rat live [17]. ROS generated by Nox4 was shown to exacerbate mitochondrial ROS production and induce mitochondrial dysfunction [18-20]. We further showed that overexpression of manganese superoxide dismutase (SOD2) decreased fluoride-induced mitochondrial ROS levels and that this protects against oxidative damage and mitochondrial dysfunction [21]. We therefore hypothesized that NaF might induce mitochondrial ROS in liver cells and that scavenging mitochondrial ROS could be an effective strategy in preventing NaF-induced hepatotoxicity.

Melatonin and its metabolites are powerful antioxidants and free radical scavengers [22]. Due to its amphiphilic nature, melatonin can easily penetrate all morphophysiological barriers and enter all subcellular compartments [23].

Melatonin could interact with mitochondria to maintain mitochondrial ROS homeostasis [24], and it has been reported to be protective against NaF-induced hepatotoxicity [25], and the beneficial effects may be attributed to its anti-oxidative properties and activity against mitochondrial dysfunction. However, the potential effects and underlying mechanisms are still unclear.

Sirtuin 3 (Sirt3), a nicotinamide adenine dinucleotide ($NAD^+$)-dependent deacetylase, is abundantly expressed in the liver. As the primary mitochondrial deacetylase, Sirt3 regulates the mitochondrial function via the deacetylation of key energy metabolic enzymes as well as antioxidant enzymes, SOD2 [26, 27]. Within the mitochondrial matrix, SOD2 is the main enzyme responsible for scavenging harmful superoxide ($O_2^{\bullet-}$) [28] and is also a substrate of Sirt3, the physical binding of Sirt3 with SOD2 results in the deacetylation and activation of SOD2 [29]. Moreover, Sirt3 can interact with forkhead box O3a (FoxO3a) in mitochondria and activate the FoxO3a-dependent antioxidant-encoding SOD2 expression [30], and thereby, inhibiting oxidative damage. Therefore, the aims of this study were to evaluate the protective effect of melatonin on NaF-induced hepatotoxicity and the role of Sirt3 signaling in this process.



## Materials and methods

### Ethics statement

This study was performed in strict accordance with the guidelines for the care and use of animals of Northwest A&F University. All animal experimental procedures were approved by the Animal Care Commission of the College of Veterinary

Medicine, Northwest A&F University.

**Cell culture, reagents, and transient plasmid transfection**

The normal human liver L-02 cells were purchased from Chinese Center for Type Culture Collection, Wuhan University. The cells were cultured in Dulbecco's Modified Eagle's Medium (DMEM, Gibco, USA), which was supplemented with 10 % heat-inactivated fetal bovine serum (FBS, Gibco) in a 5% $CO_2$ humidified atmosphere at 37°C. Sodium fluoride (NaF) and melatonin (N-acetyl-5-methoxytryptamine) were obtained from Sigma-Aldrich (St. Louis, MO, USA) and dissolved in distilled water and in absolute ethanol, respectively. The working concentration were as follows: 2 mM NaF and 40 μM melatonin (unless stated otherwise). The mitochondrial permeability transition pore inhibitor cyclosporine A and the mitochondrial K-ATP channel activator diazoxide were purchased from Selleck Chemicals (Houston, TX, USA). Specific pathway inhibitors LY294002 and SP600125 were purchased from Cell Signaling Technology (Danvers, MA, USA). The standard stock and trial solutions were prepared according to the manufacturer's instructions. Caspase-3 inhibitor [Z-Asp(O-Me)-Glu(O-Me)-Val-Asp(O-Me) fluoromethyl ketone (Z-DEVD- fmk)], control siRNA, and siRNA targeting Sirt3, NADPH Oxidase 4 (Nox4), Superoxide Dismutase 2 (SOD2), peroxisome proliferator-activated receptor gamma coactivator 1α (PGC-1α), estrogen related receptor alpha (ERRα), nuclear respiratory factor 1 (NRF1), tumor suppressor p53 (p53), and melatonin receptor (MT)-1 were purchased was obtained from Santa Cruz Biotechnology (Santa Cruz, CA, USA).

siRNAs were transfected with Lipofectamine RNAiMax reagent (Thermo Fisher Scientific) according to the manufacturer's instructions. Plasmids were transfected with Lipofectamine 3000 reagent (Thermo Fisher Scientific), according to the manufacturer's instructions.

**Cell viability**

Cell viability was measured by the Cell Counting Kit-8 Assay (Beyotime, Jiangsu, China) according to the manufacturer's protocol. The absorbance was measured using a microplate reader (Epoch, BioTek, Luzern, Switzerland) at a wavelength of 450 nm. The percentage of living cells was calculated by the ratio of the optical density of the experimental cells to that of the normal cells.

**Mitochondrial $O_2^{\bullet-}$ assessment**

The mitochondrial $O_2^{\bullet-}$ generation was assessed using the MitoSOX Red (Invitrogen), a highly selective fluorescent probe for the detection of $O_2^{\bullet-}$ generated within mitochondria. MitoSOX Red (10 μM) was incubated for 20 min in dark at 37°C to of load L-02 cells for measurement of mitochondrial $O_2^{\bullet-}$, followed by 2 washes, with Hanks Balanced Salt Solution. The fluorescence intensity was measured with an Infinite™ M200 Microplate Reader (Tecan, Mannedorf, Switzerland) and images were visualized by a Nikon eclipse Ti-S microscope equipped with the 198 Nikon DS-Ri1 digital camera (Nikon) with excitation and emission wavelengths of 492 and 595 nm, respectively.

**Determination of oxidative stress levels**

The oxidative stress levels were measured by using

2,7-dichlorodihydro-fluoresceindiacetate (DCFDA, Invitrogen) as an indicator. Briefly, cells were incubated with 5 μM DCFCA for 30 min at 37 °C, washed gently three times with warm buffer. The fluorescent product formed was quantified by spectrofluorometer using excitation/emission of 488/525 nm.

Commercial kits purchased from Nanjing Jiancheng Bioengineering Institute (Nanjing, China) were used to determine the levels of glutathione (GSH), malondialdehyde (MDA), and protein carbonyl. All procedures were conducted in accordance with the manufacturer's instructions.

**Determination of apoptotic cell death**

Cell apoptosis was detected with the Annexin V-fluorescein isothiocyanate (FITC) Apoptosis Detection kit (Beyotime) and analyzed on the BD LSR II flow cytometry system (Becton Dickinson, Franklin Lakes, NJ, USA). The total apoptosis rate of cells was calculated as the sum of the rates of cells observed in the lower-right quadrant and the upper-right quadrant.

**Caspase-3 activity**

Caspase-3 activity was measured using a commercial caspase-3 Activity Assay Kit (Beyotime) following the manufacturer's instructions. Caspase-3 activity was evaluated by enzymatic cleavage of chromophore p-nitroanilide from the substrate N-acetyl-Asp-Glu-Val-Asp-p-nitroanilide at 405 nm.

**Separation of cytosolic and mitochondrial fractions.**

Mitochondria were immediately extracted as previously described [31] using a commercial mitochondrial fractionation isolation kit (Beyotime). Mitochondrial

quantification was performed by quantifying the protein content using a BCA Protein Assay Kit (Pierce Biotech, Rockford, IL, USA). The mitochondrial fractions and the cytoplasmic fractions were aliquoted and stored at -80 °C.

**Western blotting**

Western blotting analysis was performed as has been described [32]. Briefly, equal amounts of protein sample were fractionated by SDS-PAGE and transferred to polyvinylidene difluoride (PVDF) membranes, which were blocked for 1 h with 5% (w/v) non-fat milk. The membranes were then incubated with primary antibodies at 4 °C overnight, followed by corresponding secondary antibodies for 1 h at ambient temperature. The blots were probed with 1:1000 rabbit anti-Bax, 1:1000 rabbit anti-Bcl-2, 1:1000 rabbit anti-cytochrome ***c***, 1:1000 rabbit anti-caspase-3, 1:5000 rabbit anti-COX IV, 1:3000 rabbit anti-GAPDH, 1:1000 rabbit anti-Sirt3, 1:1000 rabbit anti-SOD2, 1:1000 rabbit anti-acetylated-lysine, 1:1000 rabbit anti-p53 (Cell Signaling Technology), 1:500 rabbit anti-AKT (Thermo Fisher Scientific), 1:1000 rabbit anti-Nox4, 1:500 rabbit anti-PGC-1α, 1:1000 rabbit anti-SOD2, 1:1000 rabbit anti-SOD2 (acetyl K68), 1:1000 rabbit anti-FoxO3a, 1:1000 rabbit anti-melatonin Receptor 1A (MT1), 1:100 rabbit anti-melatonin Receptor 1B (MT2, Abcam). All phospho-antibodies were purchased from Cell Signaling Technology and diluted according to the manufacturer's instructions. Immunoblots were revealed by autograph using SuperSignal West Pico substrate (Thermo Fisher Scientific).

**Sirt3 activity**

Protein was extracted with a mild lysis buffer (50 mM Tris-HCl, pH 8; 125 mM

NaCl; 1 mM DTT; 5 mM $MgCl_2$; 1 mM EDTA; 10% glycerol; 0.1% NP-40). Sirt3 activity was determined with the CycLex Sirt3 Deacetylase Fluorometric Assay Kit according to the manufacturer's instructions (MBL International Corp. Tokyo, Japan). The fluorescence intensity was monitored at excitation and emission wavelengths of 355 and 460 nm, respectively.

**Mitochondrial membrane potential**

Mitochondrial membrane potential was detected with the fluorescent, lipophilic dye, JC-1 (BioVision, Milpitas, CA, USA) as previously described [33]. A green fluorescent JC-1 probe exists as a monomer at low membrane potentials; however, at higher potentials, JC-1 forms red-fluorescent 'J-aggregates'. The cells were incubated with 5 mg/L JC-1 for 1 h in dark, washed twice with PBS and resuspended in the serum-free medium. The ratio of red fluorescence (JC-1 J-aggregates) and green (JC-1 monomers)were measured within randomly selected cells. The mitochondrial membrane potential was represented as the ratio of red to green fluorescence intensity.

**SOD2 activity**

SOD2 activity was assayed with the Cu/Zn-SOD and Mn-SOD Assay Kit (Jiancheng Bioengineering) following the manufacturer's instructions. Cells were collected and lysed. Potassium cyanide at 3 mM was used to inhibit Cu/Zn-SOD and thus measure only MnSOD activity. After sample and SOD standard were prepared and added into 96-well plate, we initiated the reaction by adding 20 μl of diluted xanthine oxidase to all the wells. The plate was incubated on a shaker for 30

min at room temperature. The OD values were detected using a spectrophotometer at 450 nm.

**Immunoprecipitation**

Immunoprecipitation was conducted according to previously described methods with a few modifications [34]. Mitochondrial proteins (150 μg) were incubated overnight at 4°C with 5 μg of the targeted antibodies in a total volume of 250 μl. Following addition of fresh protein A/G-conjugated beads (Santa Cruz) and rotated overnight at 4°C. Finally, the beads were washed thrice with the same lysis buffer, eluted with the sample loading buffer, and analysis by SDS-PAGE.

**Construction of plasmids**

The full length coding sequences of Sirt3, nuclear respiratory factor 1 (NRF1) and estrogen-related receptor alpha (ERRα) were amplified from L-02 cDNA, then the sequences were inserted into pCMV-HA plasmid by molecular cloning methods and confirmed by sequencing. All the primers used for plasmids are listed in Supplementary Tables 1 and 2.

Sirt3 promoters were cloned from genomic DNA of L-02 cells by polymerase chain reaction (PCR). P-2kb, P-1.5kb, P-1 kb, and P-0.5kb constructs containing the Sirt3 promoter regions –2,092 to + 144 bp (relative to transcription start site), –1,458 to + 144 bp, –864 to + 144 bp, and –348 to + 144 bp were amplified using the different forward primers and common reverse primer. All these plasmids were confirmed by sequencing. All the primers used for plasmids are listed in Supplementary Tables 3 and 4.

**Quantitative Real-time PCR (qPCR) analysis**

Total RNA was isolated with the TRIzol Reagent (Invitrogen), which was reverse transcribed to cDNA with the SYBR PrimeScript RT-PCR Kit (Takara BIO Inc., Japan). The gene-specific primers used are listed in Supplementary Table 5. Results were normalized to levels of GAPDH mRNA and expressed as the fold change ($2^{-\Delta\Delta Ct}$).

**Luciferase reporter assay**

The cell signaling pathway profiling systems used in this study were commoditized products that purchased from Clontech (TaKaRa-Clontech, Tokyo, Japan). Supplementary Table 6 shows the plasmids used and the pathways they represent. Luciferase measurements were performed with the dual luciferase reporter (DLR) Assay System (Promega, Madison, WI, USA). Briefly, cells were transfected with 2 μg of reporter plasmid/well and 0.1 μg of *Renilla* luciferase plasmid pRL-SV40 (Promega) was co-transfected as an internal control. Data were collected with a VICTOR X5 Multilabel Plate Reader (PerkinElmer). Relative luciferase activities were measured by firefly luciferase luminescence divided by Renilla luciferase luminescence.

**Chromatin immunoprecipitation assay (ChIP)**

A ChIP assay was performed with the Pierce Agarose ChIP Kit as our previously described [35]. Briefly, cells were cross-linked with formaldehyde for 15 min at room temperature followed by glycine treatment to stop the cross-linking. Genomic DNA was isolated and sheared by ultrasonic waves and 10 % of the supernatant was

regarded as input. Antibodies against FoxO3a (Abcam) or ERRα (Cell Signaling Technology) were used for IP. The ChIP enrichment was determined with an ABI StepOnePlus PCR system (Applied Biosystems). Primer sequences used for ChIP-qPCR are listed in Supplementary Table 7.

**Electrophoretic mobility shift assay (EMSA)**

The EMSA assay was strictly performed with an Electrophoretic Mobility Shift Assay Kit (Molecular Probes, Invitrogen) according to the manufacturer's recommendations. The complementary oligonucleotides were annealed in annealing buffer (10 mM Tris-Cl, pH 7.5, 1 mM EDTA, 100 mM NaCl) to form double-stranded oligodeoxynucleotide probes. A total of 50 ng probes was incubated with 10 μg cell lysates from L-02 cells for 30 min at room temperature. For supershift experiments, ERRα monoclonal antibody was incubated with cell lysates for 30 min at room temperature, followed by incubation with probes for an additional 30 min. Then, the mixtures were resolved on 6% nondenaturing polyacrylamide gels. Primer sequences used for EMSA are listed in Supplementary Table 8.

**Animal studies**

A total of 40 two-mo-old Kunming mice were purchased from the experimental animal center of the Fourth Military Medical University. The mice were kept in standard animal housing at 22 ± 2 °C with ventilation and hygienic conditions, as well as free access to food and water. All mice except control were injected intraperitoneally with NaF (8 mg/kg) for 14 d [21]. Some mice were

intraperitoneally injected with melatonin (5 mg/kg) [36] at 2 h before NaF treatment. The control mice received an equal volume of normal saline. The livers were homogenized using an automatic homogenizer, and centrifuged at 1, 500×g for 20 min at 4°C. The supernatant was kept at –80°C until further analysis.

**Liver function**

Liver function was evaluated by measuring serum alanine aminotransferase (ALT) and aspartate aminotransferase (AST) with an automated chemistry analyzer (Olympus AU1000, Olympus, Tokyo, Japan).

**Measurement of ROS generation in isolated mitochondria**

Mitochondria were isolated from freshly harvested liver as described previously [37]. The isolated mitochondria were further purified using Percoll density gradient centrifugation. The freshly isolated mitochondria (10 μg) was incubated with pyruvate/malate(5/5 mmol/L) in a reaction buffer containing Amplex Red (0.05 mmol/L, Life Technologies) at 37°C. The fluorescent signals were monitored by spectrofluorometer at 520/580nm for every10 min.

**Statistical analysis**

Raw data were analyzed with the SPSS 19.0 software (Chicago, IL, USA). Results are expressed as mean ± SD from triplicate parallel experiments unless otherwise indicated. Statistical analyses were performed with one-way ANOVA, followed by post hoc least significant difference tests. Values with $P<0.05$ were considered statistically significant.

**Results**

**Melatonin ameliorates NaF-induced mitochondrial ROS generation and oxidative stress in human normal liver L-02 cells**

As shown in Figure 1A, NaF decreased cell viability in a dose- and time-dependent manner in L-02 cells. The cell viability was reduced to 54.3 ± 2.8% when treated with 2 mM NaF for 12 h compared to the control group. Treatment of 40 μM melatonin exhibited optimal beneficial effect on cell viability in NaF treated L-02 cells ($P$<0.01; Fig. 1B). Thus, melatonin at the concentration of 40 μM without obvious cytotoxicity was selected for subsequent assessments. A significant elevation ($P$<0.01) of MitoSOX fluorescence (an indicator of mitochondrial superoxide, Fig. 1C) and DCFDA fluorescence (an indicator of total cellular ROS, Fig. 1D) were detected in NaF-treated L-02 cells and they were suppressed to a considerable extent by pretreatment with melatonin. Notably, NaF induced MitoSOX and DCFDA fluorescence could also be attenuated by diazoxide (200 μM), an activator of the mitochondrial K-ATP channel or cyclosporine A (1 μM), an inhibitor of the mitochondrial permeability transition pore (Supplementary Figs. 1A and B), further supporting mitochondrial mechanisms of ROS induction (see discussion).

The GSH level is frequently used as an indicator of oxidative stress [38]. Decreased GSH level was observed in NaF-treated L-02 cells. However, pretreatment with melatonin restored NaF-induced change in GSH level (Fig. 1E), indicating the ameliorative effects of melatonin on NaF-induced oxidative stress. Lipid peroxidation (in terms of MDA levels) and protein carbonyl content are common

markers of cell membrane damage and oxidative modification of proteins respectively. NaF increased the levels of MDA and protein carbonylation in L-02 cells. Treatment with melatonin substantially reduced the levels of lipid peroxidation (Fig. 1F) and protein carbonylation (Fig. 1G). These results established melatonin as an effective antioxidant against NaF-induced oxidative stress.

Excessive mitochondrial ROS is well known to induce apoptosis [39]. Flow cytometric analysis demonstrated that melatonin protected L-02 cells against NaF-induced apoptosis (Fig. 2A). As shown in Figure 2B, cytochrome *c* content in the cytoplasm was higher in the NaF group compared with the control group. Melatonin pretreatment remarkably decreased the cytosolic expressions of cytochrome *c* in NaF-treated L-02 cells. The expression of Bax was increased substantially in the cytosolic fraction (Fig. 2C) but decreased substantially in the mitochondrial fraction (Fig. 2D) when cells treated with 2 mM NaF, compared with the control group. Interestingly, though Bcl-2 decreased in the cytosolic fraction as a result of NaF treatment, there seemed no significant changes ($P>0.05$) of Bcl-2 expressions in the mitochondrial fractions. Melatonin pretreatment inhibited NaF-induced changes of Bax/Bcl-2 ratio in the cytosolic and mitochondrial fractions. Because caspase-3 is a key regulator of both extrinsic and intrinsic apoptosis pathway [40] and NaF-driven apoptosis is mediated by stimulating the extrinsic apoptosis pathway while enhancing the intrinsic apoptosis pathway in hepatocytes [41, 42], we hypothesized that caspase-3 may be a positive regulator of

NaF-induced apoptosis. The induction of apoptosis (Supplementary Fig. 2) were abolished by pre-incubation with the caspase-3 inhibitor, Z-DEVE-fmk (20 μM; 2 h), suggesting that NaF-induced apoptosis proceeds via caspase-3-dependent pathway in L-02 cells. Pretreatment with melatonin reduced NaF-induced cleaved caspase-3 protein levels (Fig. 2E). Therefore, the protective effect of melatonin in hepatocytes can be attributed to reduced rates of apoptosis following NaF stimuli. Furthermore, cells were preincubated with Mito-Tempo (a mitochondria-targeted SOD mimetic) before NaF exposure. Mito-Tempo enhanced SOD2 activity (Supplementary Fig. 3A) but not SOD2 levels (Supplementary Fig. 3B), suppressed mitochondria $O_2^{\bullet-}$ level (Supplementary Fig. 3C), and decreased the NaF-mediated increase in protein carbonyl content (Supplementary Fig. 3D) and apoptosis (Supplementary Fig. 3E). Moreover, NaF-induced decrease in cell viability was markedly attenuated after treatment with Mito-Tempo (Supplementary Fig. 3F). These results confirmed that inhibiting mitochondrial $O_2^{\bullet-}$ level could rescue NaF-induced hepatotoxicity.

Recent literatures reported that Nox4 primarily expressed in liver promotes mitochondrial $O_2^{\bullet-}$ production and plays a crucial role in the pathology of NaF-induced hepatic dysfunction [17]. Western blot analysis revealed that Nox4 localize within the mitochondria in L-02 cells (Supplementary Fig. 4A) and NaF exposure increased the Nox4 expression (Fig. 3A). Knockdown of Nox4 reversed NaF-induced elevation of mitochondrial $O_2^{\bullet-}$ production (Fig. 3B) and protected L-02 cells against NaF-induced oxidative injury (Fig. 3C) and mitochondrial

dysfunction (Fig. 3D). In addition, silence of Nox4 dramatically prevented NaF-induced apoptosis (Fig. 3E). These data suggest that NaF-induced Nox4 expression promotes mitochondria $O_2^{\bullet-}$ production and induces mitochondrial dysfunction. Melatonin pretreatment attenuated Nox4 upregulation in NaF-treated L-02 cells (Fig. 3A).

**Melatonin reduces NaF-induced mitochondrial $O_2^{\bullet-}$ level by the Sirt3-mediated upregulation of SOD2**

As the main mitochondrial deacetylase, Sirt3 modulates various proteins to control mitochondrial function and oxidative stress response [43]; therefore, we investigate the effect of melatonin on Sirt3. To test this idea, Sirt3 was knockdown before melatonin treatment. Melatonin restored the NaF-mediated reduction in Sirt3 protein expression (Fig. 4A) and activity (Fig. 4B). Silencing of Sirt3 sharply abolished these effects. Melatonin-triggered decrease in mitochondrial $O_2^{\bullet-}$ production (Fig. 4C) was reversed by Sirt3 depletion. Moreover, depletion of Sirt3 with siRNA eliminated the effects of melatonin on mitochondrial membrane potential (Fig. 4D). In addition, melatonin-induced increase in cell viability was significantly decreased ($P$<0.01; Fig. 4E) by knocking down of Sirt3.

SOD2 is the mitochondrial antioxidant that aids in the elimination of $O_2^{\bullet-}$, and is a substrate of Sirt3 in mitochondria. As shown in Figures 5A and B, the upregulated level and activity of SOD2 by melatonin were attenuated by Sirt3 deficiency. Notably, melatonin-triggered decrease in Nox4 expression was reserved by SOD2 depletion (Fig. 5C), suggesting a potential interaction between mitochondrial $O_2^{\bullet-}$

and Nox4 activation. SOD2 activity is tightly regulated by acetylation at its lysine residues [44]. Given the apparent link between Sirt3 and SOD2, we explored the relationship between the influence of melatonin on Sirt3 and SOD2 activity. Coimmunoprecipitation pull-down (Co-IP) assay results indicated that melatonin promoted the binding of SOD2 and Sirt3 in mitochondria (Fig. 5D), and resulted in the decreased acetylation of SOD2 (Fig. 5E). Sirt3 knockdown diminished the effects of melatonin on the deacetylation levels of SOD2 (Fig. 5F). Overexpression of Sirt3 alleviated NaF-induced suppression of Sirt3 activity (Supplementary Fig. 5A) and expression (Supplementary Fig. 5B). Moreover, Sirt3 overexpression decreased the expression of acetylated-SOD2 induced by NaF in L-02 cells (Supplementary Fig. 5C). However, the deacetylase-deficient Sirt3 mutant (H248Y) completely eliminated the effects of Sirt3 on the deacetylation of SOD2. Collectively, these data suggest that the deacetylation of SOD2 induced by melatonin is mediated by Sirt3 and melatonin enhances SOD2 activity through the deacetylation of Sirt3.

**Melatonin upregulates SOD2 expression through the interaction of Sirt3 with FoxO3a**

It has been reported that FoxO3a plays an important role in regulating the SOD2 expression [45]. As shown in Figure 6A, FoxO3a localized in mitochondria and melatonin had little influence on the total protein level of FoxO3a. However, melatonin promoted the interaction of FoxO3a with Sirt3 in mitochondria (Fig. 6B). Loss of Sirt3 diminished melatonin-mediated deacetylation of FoxO3a (Fig. 6C).

Moreover, the FoxO3a-luciferase reporter plasmid (containing FoxO3a-binding motifs cAGGCTGGGCGGCGGgagctcacgcgtCCGCGAAGAAACgctagcctcgagCCTCCTGGCTTTa) assay indicated that melatonin increased the transcriptional activity of FoxO3a, whereas the regulative activities of melatonin were abolished when the cells were co-transfected with the Sirt3 siRNA and FoxO3a-luciferase plasmid (Fig. 6D) verify that FoxO3a physically occupies the SOD2 promoter, we performed the ChIP assay. As shown in Figure 6E, melatonin promoted the binding of FoxO3a to the promoter of SOD2. We also examined the expression of catalase, another downstream target of FoxO3a, and found that melatonin had no effect on catalase expression in L-02 cells (data not shown).

Overexpression of Sirt3, not Sirt3$^{H248Y}$, suppressed the acetylation of FoxO3a in cells exposed to NaF (Supplementary Fig. 6A). As a result, enhancing the transcriptional activity of FoxO3a (Supplementary Fig. 6B). These results indicate that melatonin enhances SOD2 expression by promoting Sirt3-modulated FoxO3a transcriptional activity.

**Melatonin upregulates Sirt3 via activation of PGC-1α-dependent ERRα signaling pathway**

As shown in Figure 7A, PGC-1α siRNA transfection prevented the induction of Sirt3 expression induced by melatonin, indicating that PGC-1α was required for Sirt3 expression. It has been demonstrated that ERRα, NRF1, or NRF2 not only act as the downstream targets of PGC-1α, but is also co-activated by this transcriptional

coactivator [46]. Here, we found that PGC-1α interacted with NRF1 and ERRα in L-02 cells (Supplementary Fig. 7A). To find the transcription factor of Sirt3, we performed overexpression and knockdown of NRF1 or ERRα. PGC-1α overexpression increased Sirt3 expression and cotransfection of PGC-1α and ERRα could increase more expression of Sirt3 (Fig. 7B). While, ERRα or NRF1 overexpression alone had no effect on Sirt3 expression (Fig. 7C and supplementary Fig. 7B). Overexpression of ERRα, not NRF1, followed by melatonin treatment could increase more Sirt3 mRNA levels compared with melatonin treatment alone (Fig. 7D and supplementary Fig. 7C). Moreover, melatonin-induced upregulation of Sirt3 mRNA was completely reversed by knocking down ERRα (Fig. 7E). By contrast, melatonin treatment increased Sirt3 mRNA expression, and this phenomenon persisted, even after NRF1 knockdown (Supplementary Fig. 7D). These results suggested that melatonin activated Sirt3 mRNA transcription via a PGC-1α-dependent ERRα-mediated signaling pathway.

Subsequently, –2092 bp to +144 bp Sirt3 promoter region was amplified by PCR for genomic DNA of L-02 cells, and then a series of truncated segments of the promoter were inserted into pGL4.10 for DLR assay to confirm the foregoing conclusion. As shown in Figure 8A, upon deletion of the promoter region of –2092 bp to –864 bp, the Sirt3 promoters activities were upregulated by melatonin treatment. However, melatonin lost its ability to regulate Sirt3 promoter activity following deletion of –864 bp to –348 bp. Therefore, the sequence between –864 bp to –348 bp was analyzed, and a ERRE-intensive area (TGCCATTG) was revealed

at position –497 bp/–490 bp upstream of the transcriptional start site. In addition, we compared this motif and its flanking sequence of the Sirt3 promoter with corresponding promoter sequences from different species, including mouse and chimpanzee. Based on the sequence alignment, the putative ERR binding site is evolutionarily conserved (Fig. 8B).

Next, –864 bp to +144 bp Sirt3 promoter region was cloned into the luciferase reporter vector, pGL4.10 (P-WT), and the potential ERR binding element was mutated to CTACAGGT (P-MUT; primer sequences are listed in Supporting information Table 4). DLR assays were performed to confirm that this mutated residue is responsible for response to melatonin signaling. As shown in Figure 8C, the p-WT group gave good reproducibility in response to melatonin, NaF, or PGC-1α knockdown; whereas this effect was almost completely abolished in p-MUT group. These data revealed that the –497 bp to –490 bp fragment of the Sirt3 promoter is responsible for response to the melatonin-mediated ERRα signaling.

EMSA assay was then performed to test the in vitro binding of ERRα and the –497 to –490 bp Sirt3 fragment. The sequence “gctagTGCCATTGcgtcat” repeat was used as a WT nucleic acid probe, and the sequence (TGCCATTG) mutated to CTACAGGT was used as MUT probe. A preliminary experiment was performed to test the binding of probe (Fig. 8D-left). As shown in Figure 8D-middle, there was a shift band in the lane loaded with WT probe and lysates compared with lysates alone. The protein–probe binding was regulated by NaF and melatonin, as expected.

Moreover, a specific super-shift band was detected with the ERRα antibody, thereby indicating that ERRα was bound to the probe (Fig. 8D-right).

To further confirm the EMSA results and to verify that ERRα physically occupies the Sirt3 promoter, we performed the ChIP assay. As shown in Figure 8E, a 4.7-fold enrichment of ERRα was observed. Collectively, these results suggest that ERRα directly binds to the Sirt3 promoter and activates the expression of Sirt3.

**Melatonin upregulates PGC-1α expression through the activation of MT1-PI3K/AKT signaling pathway**

Recently, adenosine monophosphate-activated protein kinase (AMPK) has been reported to function as the critical upstream signaling of PGC-1α [47-49]. However, melatonin treatment did not alter AMPK signaling (Supplementary Fig. 8A). To investigate the mechanism of melatonin-induced PGC-1α activation, the cell signaling pathway profiling systems were used. Melatonin treatment affected 5 of 12 pathways (Fig. 9A). Then the specific inhibitors of these 5 pathways were used to determine those involved in PGC-1α regulation. Melatonin-triggered AKT activation was inhibited in L-02 cells pretreated with LY294002 (a PI3K/AKT-specific inhibitor), accompanied by decreased PGC-1α expression (Fig. 9B) and Sirt3 promoter activity (Fig. 9C). Hence, melatonin exerts its effect mainly through the PI3K/AKT signaling pathway.

In mammals, melatonin exerts numerous biologic function via the 2 receptors of the G-protein-coupled superfamily: MT1 and -2. Our data show that only the MT1 membrane receptor was detected in L-02 cells (Supplementary Fig. 8B). The role of

MT1 was further evaluated by the use of an melatonin receptor antagonist and MT1 siRNA transfection. Chemical inhibition of MT1 decreased the phosphorylated AKT and PGC-1α expression (Fig. 10A), as well as the Sirt3 promoter activity (Fig. 10B). Hence, melatonin upregulates Sirt3 expression, mainly by activating MT1.

**Melatonin attenuates NaF-induced JNK1/2 activation in mice liver**

To determine whether melatonin suppressed NaF-induced oxidative stress *in vivo*, we examined the effects of melatonin in mouse model. NaF resulted in liver damage, which was confirmed by increases in serum activities of ALT and AST were significantly attenuated ($P$<0.01) by melatonin therapy (Supplementary Figs. 9A and B). Melatonin increased phosphorylated-AKT, PGC-1α, Sirt3, and SOD2 expression (Supplementary Fig. 9C). Meanwhile, NaF-induced upregulation of Nox4 and acetylated-SOD2 (acetyl K68) were also modulated by melatonin (Supplementary Fig. 9C). Moreover, administration of melatonin abolished NaF-induced mitochondrial ROS generation and oxidative injury in mice liver (Supplementary Figs. 9D-F).

Apoptosis plays an important role in the pathogenetic mechanisms involved in fluorosis. As shown in Figures 11A and B. NaF treatment decreased Bcl-2/Bax ratio and increased caspase-3 activity, which could be reversed by melatonin. Since activation of mitogen-activated protein kinases (MAPKs) have been implicated in apoptosis and they are sensitive to oxidative stress [50]. Western blot analysis showed that phosphorylated JNK1/2 was increased in NaF-exposed mice liver (Fig. 11A) while no changes in phosphorylated ERK1/2 and p38 were observed (data not

shown). Melatonin suppressed JNK1/2 phosphorylation in NaF-induced mice liver. *In vitro,* NaF treatment also increased phosphorylation of JNK1/2. To further address the involvement of JNK1/2, L-02 cells were pretreated with melatonin or SP600125 (a potent JNK1/2 inhibitor) followed by NaF treatment. NaF increased phosphorylated JNK1/2, which was abolished by melatonin or SP600125 (Fig. 11C). In addition, SP600125 prevented NaF-induced apoptosis (Figs. 11D and E).

**Discussion**

Our study provides direct evidence that protection from mitochondrial $O_2^{\bullet-}$ by melatonin confers resistance to NaF-induced hepatotoxicity. Further investigation reveals the key role of mitochondrial Sirt3 in the regulation of mitochondrial $O_2^{\bullet-}$ levels in melatonin-treated liver cells. Melatonin not only enhances the activity of SOD2 via enhancing Sirt3-mediated deacetylation, but also increases SOD2 expression by promoting the transcriptional activity of FoxO3a. Most importantly, the results of this study, for the first time, support a model whereby melatonin activates MT1-PI3K/AKT-PGC-1α signaling, which is required for ERRα-dependent Sirt3 transcription.

Mitochondria are the main producers of ROS and that the toxicity of fluoride is closely associated with mitochondrial ROS induction [2]. Indeed, one potential mechanisms of NaF-induced mitochondrial ROS could be the ROS-induced ROS release from mitochondria, which might be mediated by suppression of mitochondrial ATP-sensitive $K^+$ ($K_{ATP}$) channels (activated by diazoxide) or by activation of mitochondrial permeability transition pore (inhibited by cyclosporine

A) [51, 52]. As confirmed by observations that mitochondrial ROS induced by NaF was reduced by treatment with diazoxide or cyclosporine A; thus, the involvement of ROS-induced ROS release from mitochondria should be considered as one of the primary mechanisms of NaF-induced ROS signaling in liver cells. This places mitochondria in a central position for signal amplification, and conversely, for therapeutic targeting. In keeping with this concept, targeted inhibition of mitochondrial $O_2^{\bullet-}$ by Mito-Tempo efficiently mitigated oxidative damage and apoptosis in NaF-stimulated liver cells, demonstrating that maintain mitochondrial $O_2^{\bullet-}$ at tolerable levels may be a viable strategy to treat NaF-induced hepatotoxicity. The concentration of melatonin in mitochondria is extremely higher than that in other parts of the cells, and that melatonin should be classified as a mitochondrial-targeted antioxidant [53, 54]. Recent studies have focused on the role of melatonin in the regulation of mitochondrial ROS in healthy and disease states [24, 55]. Sirt3, Sirt4, and Sirt5 are the three sirtuin family members that are mainly localized to the mitochondria. Among them, Sirt3 is the most robust acetyl-lysine deacetylase in mitochondria that control the mitochondrial ROS elimination [56-58]. Accumulating evidence suggests that melatonin and Sirt3 both play indispensable roles in intrinsic anti-oxidative mechanisms [59]. Therefore, we paid much attention on the relationship between melatonin and Sirt3. Other report including the present study showed that melatonin can up-regulate Sirt3 expression in liver cells and in turn attenuate NaF-induced rise in mitochondrial $O_2^{\bullet-}$ [48]. Blocking Sirt3 by siRNA abolished the liver cell protection conferred by melatonin suggesting that

melatonin acts via Sirt3 pathways.

SOD2 is a major downstream signal of Sirt3-mediated mitochondrial $O_2^{\bullet-}$ reduction and deacetylation of SOD2 by Sirt3 regulates SOD2 enzymatic activity [60, 61]. The present study shows that loss of Sirt3 diminished the melatonin-induced the decrease of the acetylated SOD2 and the upregulated expression of SOD2. In addition, several groups have provided evidence that Sirt3 promotes the transcription of SOD2 through the activation of FoxO3a [62, 63]. Melatonin promotes the interaction of FoxO3a with Sirt3 in mitochondria and enhances FoxO3a deacetylation [64], thus promoting nuclear translocation of FoxO3a. Collectively, through promoting Sirt3-modulated transcription and activity of SOD2, melatonin inhibits NaF-induced mitochondrial $O_2^{\bullet-}$ production. Moreover, recent studies have shown that Nox4 is a predominant source of ROS in hepatocytes. The present study shows that Nox4 was up-regulated in NaF-treated liver cells, which is consistent with recent report [17]. Treatment of liver cells with siRNA directed against Nox4 decreased Nox4 expression levels and reduced oxidative damage as well as generation of mitochondrial $O_2^{\bullet-}$, suggesting that Nox4 promotes mitochondrial $O_2^{\bullet-}$ generation. On the other hand, melatonin-induced inhibition of the expression of Nox4 was reversed by knocking down SOD2. This suggests that reducing mitochondrial $O_2^{\bullet-}$ by melatonin substantially attenuated NaF-induced Nox4 upregulation. In fact, this has been recognized that mitochondrial ROS positively regulates NADPH oxidase subunits expression and activation under pathological conditions [65, 66]. Thus, it is most likely that cross-talks between

mitochondria and NADPH oxidase form a positive feedback loop in favor of ROS production and oxidative damage in liver cells, and disruption of this feedback loop by inhibiting either of them provides beneficial effects on NaF-induced hepatotoxicity.

In agreement with the recent experimental data indicating increased AKT phosphorylation by melatonin [67, 68], our results further confirmed that melatonin stimulated phosphorylation of AKT in liver cells. Furthermore, we reported for the first time, that melatonin activates PI3K/AKT signaling, which is required for PGC-1α expression. PGC-1α activated the Sirt3 mRNA transcription promoter, which was mediated by an estrogen-related receptor (ERR) binding element (ERRE) mapped to the Sirt3 promoter region in liver cells. These results are supported by those of Kong and colleagues [69]. It is noteworthy that melatonin exerts numerous biologic function through specific plasma membrane receptors [70, 71]. There are two subtypes of melatonin membrane receptors (MT), MT1 and MT2, both of which are members of the seven transmembrane G protein-coupled receptor family. Only expression of the MT1 protein was found in L-02 cells. Pharmacological and genetic inhibition of MT1 abolished the effects of melatonin on AKT phosphorylation.

MAPKs are a group of protein serine/threonine kinases that play important roles in complex cellular programs and they are sensitive to oxidative stress [72], we therefore examined three subfamilies of MAPKs, including ERK1/2, JNK1/2, and p38. JNKs and p38-MAPKs were deemed to be stress responsive and thus involved

in apoptosis [73]. Our results demonstrated a direct correlation between NaF-induced apoptotic cell death and JNK-activation in liver cells. However, it is important to recognize that fluoride is a recognized GTP-binding proteins (G proteins) activator and protein phosphatase inhibitor [2, 74-76]. Fluoride activates due to the formation of an $AlF_4^-$ complex, and this leads to the subsequent activation of G protein-linked signal transduction pathway. On the other hand, the $F^-$ anion is also known as an inhibitor of protein phosphatases, thereby retaining signal molecules in an active phosphorylated state [77]. Further study needs to investigate what extent this activation is mediated via G protein activation or phosphatase inhibition. In the present study, administration of melatonin prevented NaF-induced JNK1/2 activation *in vivo* and *in vitro*, and inhibition of JNK1/2 prevented apoptosis in NaF-exposed liver cells. Thus, the attenuation of fluoride-induced JNK1/2 phosphorylation by melatonin may be one of the downstream mechanisms underlying protection by melatonin.

Since p53 is a transcriptional repressor that controls the expression of Bcl-2 [78] and NaF exposure has been shown to induce p53 expression in L-02 cells [79]. In p53 siRNA cells, the expression of the Bcl-2 was increased, and not altered after NaF exposure (Supplementary Fig. 10A). It is well established that p53 has a close relation with ROS. p53 activity can be regulated by ROS, and ROS regulate cell fate through p53 [80]. By applying Mito-Tempo (Supplementary Fig. 10B), we confirmed that ROS mediated p53 activation in L-02 cells. Therefore, the decreased Bcl-2 expression induced by NaF can be attributed to ROS-dependent p53

activation in L-02 cells. Despite the observation of oxidative stress and apoptosis increase, treatment with NaF resulted in several potentially protective responses. Most notably, NaF led to an increase in the mitochondrial Bcl-2:Bax ratio. Although it appears that both Bax and Bcl-2 can regulate apoptosis independently, there also seems to be an in vivo competition that exists between the two. Homodimers of Bax (Bax/Bax) create large pores in the outer membrane and promote apoptosis by facilitating the release of cytochrome *c*, whereas heterodimers of Bcl-2/Bax prevent pore formation and inhibit apoptosis [81]. Because cytochrome *c* was elevated in the cytosol of NaF-treated liver cells, we would have expected to see a decrease in the Bcl-2:Bax ratio. However, we found a significant decrease in mitochondrial levels of Bax in the NaF treated group and no changes in mitochondrial Bcl-2 between groups. This resulted in an increase in the Bcl-2:Bax ratio, suggesting an adaptive response may have occurred that could make cells more resistant to mitochondrial-mediated apoptosis induced by NaF and this needs further investigation.

In conclusion, we found that melatonin facilitates the expression of Sirt3 by activating the PI3K/AKT-PGC1α signaling pathway, thus protecting liver cells against from NaF-induced oxidative damage. Our findings may also provide valuable clues in the search for new drugs that can be applied to clinical application for the treatment or prevention of NaF-induced hepatotoxicity.



**Acknowledgements**

This work was supported by the National Natural Science Foundation of China (No. 31702205), Special Financial Grant for the China Postdoctoral Science Foundation (No. 2017T100781), China Postdoctoral Science Foundation Grant (No. 2016M590978), Young Talent Fund of University Association for Science and Technology in Shaanxi, China (No. 20170203) and Natural Science Basic Research Plan in Shaanxi Province of China (No. 2017JQ3028).

**Competing interests**

The authors indicate no competing financial interest.

**Author contributions**

Chao Song: Conception and design, collection and assembly of data, data analysis and interpretation, manuscript writing

Jiamin Zhao: Collection and assembly of data

Beibei Fu: Collection and assembly of data

Dan Li: Collection and assembly of data

Tingchao Mao: Collection and assembly of data

Wei Peng: Collection and assembly of data

Haibo Wu: Conception and design, collection and assembly of data, data analysis and interpretation

Yong Zhang: Conception and design, data analysis and interpretation, financial support, final approval of manuscript

**References**

[1] N. Taghipour, H. Amini, M. Mosaferi, M. Yunesian, M. Pourakbar, H. Taghipour, National and sub-national drinking water fluoride concentrations and prevalence of fluorosis and of decayed, missed, and filled teeth in Iran from 1990 to 2015: a systematic review, Environ Sci Pollut Res Int 23(6) (2016) 5077-5098.

[2] O. Barbier, L. Arreola-Mendoza, L.M. Del Razo, Molecular mechanisms of fluoride toxicity, Chem Biol Interact 188(2) (2010) 319-333.

[3] M. Suzuki, J.D. Bartlett, Sirtuin1 and autophagy protect cells from fluoride-induced cell stress, Biochim Biophys Acta 1842(2) (2014) 245-255.

[4] M. Fu, X. Wu, J. He, Y. Zhang, S. Hua, Natrium fluoride influences methylation modifications and induces apoptosis in mouse early embryos, Environ Sci Technol 48(17) (2014) 10398-10405.

[5] A. Chattopadhyay, S. Podder, S. Agarwal, S. Bhattacharya, Fluoride-induced histopathology and synthesis of stress protein in liver and kidney of mice, Arch Toxicol 85(4) (2011) 327-335.

[6] H.A. Pereira, L. Leite Ade, S. Charone, J.G. Lobo, T.M. Cestari, C. Peres-Buzalaf, M.A. Buzalaf, Proteomic analysis of liver in rats chronically exposed to fluoride, PLoS One 8(9) (2013) e75343.

[7] B.H. Zhou, J. Zhao, J. Liu, J.L. Zhang, J. Li, H.W. Wang, Fluoride-induced oxidative stress is involved in the morphological damage and dysfunction of liver in female mice, Chemosphere 139 (2015) 504-511.

[8] E. Dabrowska, M. Balunowska, R. Letko, B. Szynaka, Ultrastructural study of the mitochondria in the submandibular gland, the pancreas and the liver of young rats, exposed to NaF in drinking water, Rocz Akad Med Bialymst 49 Suppl 1 (2004) 180-181.

[9] J. Cao, J. Chen, J. Wang, R. Jia, W. Xue, Y. Luo, X. Gan, Effects of fluoride on liver apoptosis and Bcl-2, Bax protein expression in freshwater teleost, Cyprinus carpio, Chemosphere 91(8) (2013) 1203-1212.

[10] J. Ameeramja, L. Panneerselvam, V. Govindarajan, S. Jeyachandran, V. Baskaralingam, E. Perumal, Tamarind seed coat ameliorates fluoride induced cytotoxicity, oxidative stress, mitochondrial dysfunction and apoptosis in A549 cells, J Hazard Mater 301 (2016) 554-565.

[11] M. Suzuki, C. Bandoski, J.D. Bartlett, Fluoride induces oxidative damage and SIRT1/autophagy through ROS-mediated JNK signaling, Free Radic Biol Med 89 (2015) 369-378.

[12] J. Niemann, C. Johne, S. Schroder, F. Koch, S.M. Ibrahim, J. Schultz, M. Tiedge, S. Baltrusch, An mtDNA mutation accelerates liver aging by interfering with the ROS response and mitochondrial life cycle, Free Radic Biol Med 102 (2017) 174-187.

[13] P. Mahaboob Basha, S.M. Saumya, Suppression of mitochondrial oxidative phosphorylation and TCA enzymes in discrete brain regions of mice exposed to high fluoride: amelioration by Panax ginseng (Ginseng) and Lagerstroemia speciosa

(Banaba) extracts, Cell Mol Neurobiol 33(3) (2013) 453-464.

[14] L. Yan, S. Liu, C. Wang, F. Wang, Y. Song, N. Yan, S. Xi, Z. Liu, G. Sun, JNK and NADPH oxidase involved in fluoride-induced oxidative stress in BV-2 microglia cells, Mediators Inflamm 2013 (2013) 895975.

[15] J.A. Izquierdo-Vega, M. Sanchez-Gutierrez, L.M. Del Razo, NADPH oxidase participates in the oxidative damage caused by fluoride in rat spermatozoa. Protective role of alpha-tocopherol, J Appl Toxicol 31(6) (2011) 579-588.

[16] Q. Sun, W. Zhang, W. Zhong, X. Sun, Z. Zhou, Pharmacological inhibition of NOX4 ameliorates alcohol-induced liver injury in mice through improving oxidative stress and mitochondrial function, Biochim Biophys Acta 1861(1 Pt A) (2017) 2912-2921.

[17] V.V. Kanagaraj, L. Panneerselvam, V. Govindarajan, J. Ameeramja, E. Perumal, Caffeic acid, a phyto polyphenol mitigates fluoride induced hepatotoxicity in rats: A possible mechanism, Biofactors 41(2) (2015) 90-100.

[18] T. Ago, J. Kuroda, J. Pain, C. Fu, H. Li, J. Sadoshima, Upregulation of Nox4 by hypertrophic stimuli promotes apoptosis and mitochondrial dysfunction in cardiac myocytes, Circ Res 106(7) (2010) 1253-1264.

[19] J. Kuroda, T. Ago, S. Matsushima, P. Zhai, M.D. Schneider, J. Sadoshima, NADPH oxidase 4 (Nox4) is a major source of oxidative stress in the failing heart, Proc Natl Acad Sci U S A 107(35) (2010) 15565-15570.

[20] A. Shah, L. Xia, H. Goldberg, K.W. Lee, S.E. Quaggin, I.G. Fantus, Thioredoxin-interacting protein mediates high glucose-induced reactive oxygen species generation by mitochondria and the NADPH oxidase, Nox4, in mesangial cells, J Biol Chem 288(10) (2013) 6835-6848.

[21] C. Song, B. Fu, J. Zhang, J. Zhao, M. Yuan, W. Peng, Y. Zhang, H. Wu, Sodium fluoride induces nephrotoxicity via oxidative stress-regulated mitochondrial SIRT3 signaling pathway, Sci Rep 7(1) (2017) 672.

[22] M.R. Ramis, S. Esteban, A. Miralles, D.X. Tan, R.J. Reiter, Protective Effects of Melatonin and Mitochondria-targeted Antioxidants Against Oxidative Stress: A Review, Curr Med Chem 22(22) (2015) 2690-2711.

[23] C. Venegas, J.A. Garcia, G. Escames, F. Ortiz, A. Lopez, C. Doerrier, L. Garcia-Corzo, L.C. Lopez, R.J. Reiter, D. Acuna-Castroviejo, Extrapineal melatonin: analysis of its subcellular distribution and daily fluctuations, J Pineal Res 52(2) (2012) 217-227.

[24] D. Acuna Castroviejo, G. Escames, A. Carazo, J. Leon, H. Khaldy, R.J. Reiter, Melatonin, mitochondrial homeostasis and mitochondrial-related diseases, Curr Top Med Chem 2(2) (2002) 133-151.

[25] V.K. Bharti, R.S. Srivastava, H. Kumar, S. Bag, A.C. Majumdar, G. Singh, S.R. Pandi-Perumal, G.M. Brown, Effects of melatonin and epiphyseal proteins on fluoride-induced adverse changes in antioxidant status of heart, liver, and kidney of rats, Adv Pharmacol Sci 2014 (2014) 532969.

[26] H.J. Weir, J.D. Lane, N. Balthasar, SIRT3: A Central Regulator of Mitochondrial Adaptation in Health and Disease, Genes Cancer 4(3-4) (2013) 118-124.

[27] H. Pi, S. Xu, R.J. Reiter, P. Guo, L. Zhang, Y. Li, M. Li, Z. Cao, L. Tian, J. Xie, R. Zhang, M. He, Y. Lu, C. Liu, W. Duan, Z. Yu, Z. Zhou, SIRT3-SOD2-mROS-dependent autophagy in cadmium-induced hepatotoxicity and salvage by melatonin, Autophagy 11(7) (2015) 1037-1051.

[28] A. Miar, D. Hevia, H. Munoz-Cimadevilla, A. Astudillo, J. Velasco, R.M. Sainz, J.C. Mayo, Manganese superoxide dismutase (SOD2/MnSOD)/catalase and SOD2/GPx1 ratios as biomarkers for tumor progression and metastasis in prostate, colon, and lung cancer, Free Radic Biol Med 85 (2015) 45-55.

[29] X. Qiu, K. Brown, M.D. Hirschey, E. Verdin, D. Chen, Calorie restriction reduces oxidative stress by SIRT3-mediated SOD2 activation, Cell Metab 12(6) (2010) 662-667.

[30] S. Padmaja Divya, P. Pratheeshkumar, Y.O. Son, R. Vinod Roy, J. Andrew Hitron, D. Kim, J. Dai, L. Wang, P. Asha, B. Huang, M. Xu, J. Luo, Z. Zhang, Arsenic Induces Insulin Resistance in Mouse Adipocytes and Myotubes Via Oxidative Stress-Regulated Mitochondrial Sirt3-FOXO3a Signaling Pathway, Toxicol Sci 146(2) (2015) 290-300.

[31] J. Xiao, R. Zhang, F. Huang, L. Liu, Y. Deng, Y. Ma, Z. Wei, X. Tang, Y. Zhang, M. Zhang, Lychee (Litchi chinensis Sonn.) Pulp Phenolic Extract Confers a

Protective Activity against Alcoholic Liver Disease in Mice by Alleviating Mitochondrial Dysfunction, J Agric Food Chem 65(24) (2017) 5000-5009.

[32] H. Wu, Y. Wu, Z. Ai, L. Yang, Y. Gao, J. Du, Z. Guo, Y. Zhang, Vitamin C enhances Nanog expression via activation of the JAK/STAT signaling pathway, Stem Cells 32(1) (2014) 166-176.

[33] R. Ye, X. Kong, Q. Yang, Y. Zhang, J. Han, G. Zhao, Ginsenoside Rd attenuates redox imbalance and improves stroke outcome after focal cerebral ischemia in aged mice, Neuropharmacology 61(4) (2011) 815-824.

[34] L. Lai, L. Yan, S. Gao, C.L. Hu, H. Ge, A. Davidow, M. Park, C. Bravo, K. Iwatsubo, Y. Ishikawa, J. Auwerx, D.A. Sinclair, S.F. Vatner, D.E. Vatner, Type 5 adenylyl cyclase increases oxidative stress by transcriptional regulation of manganese superoxide dismutase via the SIRT1/FoxO3a pathway, Circulation 127(16) (2013) 1692-1701.

[35] L. Wei, Y. Zhou, C. Qiao, T. Ni, Z. Li, Q. You, Q. Guo, N. Lu, Oroxylin A inhibits glycolysis-dependent proliferation of human breast cancer via promoting SIRT3-mediated SOD2 transcription and HIF1alpha destabilization, Cell Death Dis 6 (2015) e1714.

[36] B. San-Miguel, I. Crespo, D.I. Sanchez, B. Gonzalez-Fernandez, J.J. Ortiz de Urbina, M.J. Tunon, J. Gonzalez-Gallego, Melatonin inhibits autophagy and endoplasmic reticulum stress in mice with carbon tetrachloride-induced fibrosis, J Pineal Res 59(2) (2015) 151-162.

[37] R. Ni, T. Cao, S. Xiong, J. Ma, G.C. Fan, J.C. Lacefield, Y. Lu, S. Le Tissier, T. Peng, Therapeutic inhibition of mitochondrial reactive oxygen species with mito-TEMPO reduces diabetic cardiomyopathy, Free Radic Biol Med 90 (2016) 12-23.

[38] C.C. Liu, J.M. Gebicki, Intracellular GSH and ascorbate inhibit radical-induced protein chain peroxidation in HL-60 cells, Free Radic Biol Med 52(2) (2012) 420-426.

[39] H. Li, W. Jiang, Y. Liu, J. Jiang, Y. Zhang, P. Wu, J. Zhao, X. Duan, X. Zhou, L. Feng, The metabolites of glutamine prevent hydroxyl radical-induced apoptosis through inhibiting mitochondria and calcium ion involved pathways in fish erythrocytes, Free Radic Biol Med 92 (2016) 126-140.

[40] Y. Shao, Z. Gao, P.A. Marks, X. Jiang, Apoptotic and autophagic cell death induced by histone deacetylase inhibitors, Proc Natl Acad Sci U S A 101(52) (2004) 18030-18035.

[41] G.H. Song, F.B. Huang, J.P. Gao, M.L. Liu, W.B. Pang, W. Li, X.Y. Yan, M.J. Huo, X. Yang, Effects of Fluoride on DNA Damage and Caspase-Mediated Apoptosis in the Liver of Rats, Biol Trace Elem Res 166(2) (2015) 173-182.

[42] K. Miao, L. Zhang, S. Yang, W. Qian, Z. Zhang, Intervention of selenium on apoptosis and Fas/FasL expressions in the liver of fluoride-exposed rats, Environ Toxicol Pharmacol 36(3) (2013) 913-920.

[43] A. Ansari, M.S. Rahman, S.K. Saha, F.K. Saikot, A. Deep, K.H. Kim, Function

of the SIRT3 mitochondrial deacetylase in cellular physiology, cancer, and neurodegenerative disease, Aging Cell 16(1) (2017) 4-16.

[44] X. Liu, L. Zhang, P. Wang, X. Li, D. Qiu, L. Li, J. Zhang, X. Hou, L. Han, J. Ge, M. Li, L. Gu, Q. Wang, Sirt3-dependent deacetylation of SOD2 plays a protective role against oxidative stress in oocytes from diabetic mice, Cell Cycle 16(13) (2017) 1302-1308.

[45] B. Fu, J. Zhao, W. Peng, H. Wu, Y. Zhang, Resveratrol rescues cadmium-induced mitochondrial injury by enhancing transcriptional regulation of PGC-1alpha and SOD2 via the Sirt3/FoxO3a pathway in TCMK-1 cells, Biochem Biophys Res Commun 486(1) (2017) 198-204.

[46] X. Zhang, X. Ren, Q. Zhang, Z. Li, S. Ma, J. Bao, Z. Li, X. Bai, L. Zheng, Z. Zhang, S. Shang, C. Zhang, C. Wang, L. Cao, Q. Wang, J. Ji, PGC-1alpha/ERRalpha-Sirt3 Pathway Regulates DAergic Neuronal Death by Directly Deacetylating SOD2 and ATP Synthase beta, Antioxid Redox Signal 24(6) (2016) 312-328.

[47] L. Yu, B. Gong, W. Duan, C. Fan, J. Zhang, Z. Li, X. Xue, Y. Xu, D. Meng, B. Li, M. Zhang, Z. Bin, Z. Jin, S. Yu, Y. Yang, H. Wang, Melatonin ameliorates myocardial ischemia/reperfusion injury in type 1 diabetic rats by preserving mitochondrial function: role of AMPK-PGC-1alpha-SIRT3 signaling, Sci Rep 7 (2017) 41337.

[48] Y. Chen, W. Qing, M. Sun, L. Lv, D. Guo, Y. Jiang, Melatonin protects

hepatocytes against bile acid-induced mitochondrial oxidative stress via the AMPK-SIRT3-SOD2 pathway, Free Radic Res 49(10) (2015) 1275-1284.

[49] Z. Wan, J. Root-McCaig, L. Castellani, B.E. Kemp, G.R. Steinberg, D.C. Wright, Evidence for the role of AMPK in regulating PGC-1 alpha expression and mitochondrial proteins in mouse epididymal adipose tissue, Obesity (Silver Spring) 22(3) (2014) 730-738.

[50] Y. Geng, Y. Qiu, X. Liu, X. Chen, Y. Ding, S. Liu, Y. Zhao, R. Gao, Y. Wang, J. He, Sodium fluoride activates ERK and JNK via induction of oxidative stress to promote apoptosis and impairs ovarian function in rats, J Hazard Mater 272 (2014) 75-82.

[51] N.R. Brady, A. Hamacher-Brady, H.V. Westerhoff, R.A. Gottlieb, A wave of reactive oxygen species (ROS)-induced ROS release in a sea of excitable mitochondria, Antioxid Redox Signal 8(9-10) (2006) 1651-1665.

[52] D.B. Zorov, M. Juhaszova, S.J. Sollott, Mitochondrial ROS-induced ROS release: an update and review, Biochim Biophys Acta 1757(5-6) (2006) 509-517.

[53] R.J. Reiter, J.C. Mayo, D.X. Tan, R.M. Sainz, M. Alatorre-Jimenez, L. Qin, Melatonin as an antioxidant: under promises but over delivers, J Pineal Res 61(3) (2016) 253-278.

[54] J.C. Mayo, R.M. Sainz, P. Gonzalez-Menendez, D. Hevia, R. Cernuda-Cernuda, Melatonin transport into mitochondria, Cell Mol Life Sci (2017).

[55] G. Petrosillo, N. Moro, F.M. Ruggiero, G. Paradies, Melatonin inhibits cardiolipin peroxidation in mitochondria and prevents the mitochondrial permeability transition and cytochrome c release, Free Radic Biol Med 47(7) (2009) 969-974.

[56] A.S. Hebert, K.E. Dittenhafer-Reed, W. Yu, D.J. Bailey, E.S. Selen, M.D. Boersma, J.J. Carson, M. Tonelli, A.J. Balloon, A.J. Higbee, M.S. Westphall, D.J. Pagliarini, T.A. Prolla, F. Assadi-Porter, S. Roy, J.M. Denu, J.J. Coon, Calorie restriction and SIRT3 trigger global reprogramming of the mitochondrial protein acetylome, Mol Cell 49(1) (2013) 186-199.

[57] T. Koyama, S. Kume, D. Koya, S. Araki, K. Isshiki, M. Chin-Kanasaki, T. Sugimoto, M. Haneda, T. Sugaya, A. Kashiwagi, H. Maegawa, T. Uzu, SIRT3 attenuates palmitate-induced ROS production and inflammation in proximal tubular cells, Free Radic Biol Med 51(6) (2011) 1258-1267.

[58] E.L. Bell, B.M. Emerling, S.J. Ricoult, L. Guarente, Sirt3 suppresses hypoxia inducible factor 1alpha and tumor growth by inhibiting mitochondrial ROS production, Oncogene 30(26) (2011) 2986-2996.

[59] M. Zhai, B. Li, W. Duan, L. Jing, B. Zhang, M. Zhang, L. Yu, Z. Liu, B. Yu, K. Ren, E. Gao, Y. Yang, H. Liang, Z. Jin, S. Yu, Melatonin ameliorates myocardial ischemia reperfusion injury through SIRT3-dependent regulation of oxidative stress and apoptosis, J Pineal Res 63(2) (2017).

[60] R. Tao, M.C. Coleman, J.D. Pennington, O. Ozden, S.H. Park, H. Jiang, H.S.

Kim, C.R. Flynn, S. Hill, W. Hayes McDonald, A.K. Olivier, D.R. Spitz, D. Gius, Sirt3-mediated deacetylation of evolutionarily conserved lysine 122 regulates MnSOD activity in response to stress, Mol Cell 40(6) (2010) 893-904.

[61] H. Kim, Y.D. Lee, H.J. Kim, Z.H. Lee, H.H. Kim, SOD2 and Sirt3 Control Osteoclastogenesis by Regulating Mitochondrial ROS, J Bone Miner Res (2016).

[62] N.R. Sundaresan, M. Gupta, G. Kim, S.B. Rajamohan, A. Isbatan, M.P. Gupta, Sirt3 blocks the cardiac hypertrophic response by augmenting Foxo3a-dependent antioxidant defense mechanisms in mice, J Clin Invest 119(9) (2009) 2758-2771.

[63] K. Du, Y. Yu, D. Zhang, W. Luo, H. Huang, J. Chen, J. Gao, C. Huang, NFkappaB1 (p50) suppresses SOD2 expression by inhibiting FoxO3a transactivation in a miR190/PHLPP1/Akt-dependent axis, Mol Biol Cell 24(22) (2013) 3577-3583.

[64] A.H. Tseng, S.S. Shieh, D.L. Wang, SIRT3 deacetylates FOXO3 to protect mitochondria against oxidative damage, Free Radic Biol Med 63 (2013) 222-234.

[65] R. Rathore, Y.M. Zheng, C.F. Niu, Q.H. Liu, A. Korde, Y.S. Ho, Y.X. Wang, Hypoxia activates NADPH oxidase to increase [ROS]i and [Ca2+]i through the mitochondrial ROS-PKCepsilon signaling axis in pulmonary artery smooth muscle cells, Free Radic Biol Med 45(9) (2008) 1223-1231.

[66] S. Dikalov, Cross talk between mitochondria and NADPH oxidases, Free Radic Biol Med 51(7) (2011) 1289-1301.

[67] Y. Zhang, Z. Wei, W. Liu, J. Wang, X. He, H. Huang, J. Zhang, Z. Yang, Melatonin protects against arsenic trioxide-induced liver injury by the upregulation of Nrf2 expression through the activation of PI3K/AKT pathway, Oncotarget 8(3) (2017) 3773-3780.

[68] U. Kilic, A.B. Caglayan, M.C. Beker, M.Y. Gunal, B. Caglayan, E. Yalcin, T. Kelestemur, R.Z. Gundogdu, B. Yulug, B. Yilmaz, B.E. Kerman, E. Kilic, Particular phosphorylation of PI3K/Akt on Thr308 via PDK-1 and PTEN mediates melatonin's neuroprotective activity after focal cerebral ischemia in mice, Redox Biol 12 (2017) 657-665.

[69] X. Kong, R. Wang, Y. Xue, X. Liu, H. Zhang, Y. Chen, F. Fang, Y. Chang, Sirtuin 3, a new target of PGC-1alpha, plays an important role in the suppression of ROS and mitochondrial biogenesis, PLoS One 5(7) (2010) e11707.

[70] K. Baba, N. Pozdeyev, F. Mazzoni, S. Contreras-Alcantara, C. Liu, M. Kasamatsu, T. Martinez-Merlos, E. Strettoi, P.M. Iuvone, G. Tosini, Melatonin modulates visual function and cell viability in the mouse retina via the MT1 melatonin receptor, Proc Natl Acad Sci U S A 106(35) (2009) 15043-15048.

[71] H. Wu, C. Song, J. Zhang, J. Zhao, B. Fu, T. Mao, Y. Zhang, Melatonin-mediated upregulation of GLUT1 blocks exit from pluripotency by increasing the uptake of oxidized vitamin C in mouse embryonic stem cells, FASEB J 31(4) (2017) 1731-1743.

[72] W. Zhang, H.T. Liu, MAPK signal pathways in the regulation of cell

proliferation in mammalian cells, Cell Res 12(1) (2002) 9-18.

[73] T. Wada, J.M. Penninger, Mitogen-activated protein kinases in apoptosis regulation, Oncogene 23(16) (2004) 2838-2849.

[74] E.V. Thrane, M. Refsnes, G.H. Thoresen, M. Lag, P.E. Schwarze, Fluoride-induced apoptosis in epithelial lung cells involves activation of MAP kinases p38 and possibly JNK, Toxicol Sci 61(1) (2001) 83-91.

[75] M. Flores-Mendez, D. Ramirez, N. Alamillo, L.C. Hernandez-Kelly, L.M. Del Razo, A. Ortega, Fluoride exposure regulates the elongation phase of protein synthesis in cultured Bergmann glia cells, Toxicol Lett 229(1) (2014) 126-133.

[76] J. Lee, Y.E. Han, O. Favorov, M. Tommerdahl, B. Whitsel, C.J. Lee, Fluoride Induces a Volume Reduction in CA1 Hippocampal Slices Via MAP Kinase Pathway Through Volume Regulated Anion Channels, Exp Neurobiol 25(2) (2016) 72-78.

[77] M. Refsnes, E.V. Thrane, M. Lag, G.H. Thoresen, P.E. Schwarze, Mechanisms in fluoride-induced interleukin-8 synthesis in human lung epithelial cells, Toxicology 167(2) (2001) 145-158.

[78] T. Miyashita, M. Harigai, M. Hanada, J.C. Reed, Identification of a p53-dependent negative response element in the bcl-2 gene, Cancer Res 54(12) (1994) 3131-3135.

[79] A.G. Wang, Q.L. Chu, W.H. He, T. Xia, J.L. Liu, M. Zhang, A.K. Nussler, X.M. Chen, K.D. Yang, Effects on protein and mRNA expression levels of p53 induced

by fluoride in human embryonic hepatocytes, Toxicol Lett 158(2) (2005) 158-163.

[80] B. Liu, Y. Chen, D.K. St Clair, ROS and p53: a versatile partnership, Free Radic Biol Med 44(8) (2008) 1529-1535.

[81] Z.N. Oltvai, C.L. Milliman, S.J. Korsmeyer, Bcl-2 heterodimerizes in vivo with a conserved homolog, Bax, that accelerates programmed cell death, Cell 74(4) (1993) 609-619.

**Figure Legends**

**Figure 1.** Melatonin inhibits fluoride-induced oxidative injury in L-02 cells. (A) Cells were treated with fluoride with different concentrations or for different time intervals, respectively. Cell viability was determined using the CCK-8 assay. (B) Confluent cells were pretreated for 2 h with various concentrations of melatonin. After removing the supernatants, cells were incubated with fresh medium in the presence or absence of fluoride (2 mM) for an additional 12 h. Cell viability was determined. Cells were pretreated with 40 μM melatonin for 2 h and then treated with or without 2 mM fluoride for an additional 12 h. (C) The mitochondrial $O_2^{\bullet-}$ levels were estimated using MitoSOX Red. (D) Intracellular ROS was detected with CM-DCFDA. The GSH level (E), MDA content (F), and protein carbonyl content (G) were determined. All results are representative of three independent experiments and values are presented as means ± SD. $^{**}P < 0.05$, $^{**}P < 0.01$. Ns, not significant. Abbreviations: F, fluoride; Mel, melatonin.

**Figure 2.** Melatonin attenuates fluoride-induced apoptosis in L-02 cells. Cells were

pretreated with 40 μM melatonin for 2 h and then treated with or without 2 mM fluoride for an additional 12 h. (A) Representative images of flow cytometric analysis by Annexin V-FITC/PI dual staining. (B) Release of cytochrome *c* from mitochondria was measured by Western analysis using an anti-cytochrome *c* antibody. The ratio of Bax/Bcl-2 in the cytosolic fraction (C) and mitochondrial fraction (D). (E) The cleaved caspase-3 protein expression levels were analyzed by Western blot. All results are representative of three independent experiments and values are presented as means ± SD. $^{**}P < 0.01$. Ns, not significant.

**Figure 3.** Melatonin reduces fluoride-induced upregulation of Nox4. Cells were pretreated with melatonin of 40 μM for 2 h, washed, and then treated with or without fluoride of 2 mM for an additional 12 h. (A) The immunoblot bands of Nox4. L-02 cells transfected with scrambled or Nox4 siRNA were treated with 2 mM of fluoride for 12 h. The mitochondrial $O_2^{\bullet-}$ level (B) and protein carbonyl content (C) were measured. (D) Quantification of mitochondrial membrane potential. (E) Caspase-3 activity was measured spectrophotometrically. All results are representative of three independent experiments and values are presented as means ± SD. $^{*}P < 0.05$, $^{**}P < 0.01$.

**Figure 4.** Melatonin alleviates fluoride-induced oxidative injury via Sirt3 pathway. Cells were transfected with Sirt3 siRNA. At 24-h post-transfection, cells were pretreated with melatonin (40 μM) for 2 h and then treated with or without fluoride of 2 mM for an additional 12 h. The Sirt3 protein expression (A) and its activity (B) were determined. (C) Mitochondrial $O_2\bullet^-$ levels. (D) Determination of

mitochondrial membrane potential. Red fluorescence was emitted by JC-1 aggregates in healthy mitochondria with polarized inner mitochondrial membranes, whereas green fluorescence was emitted by cytosolic JC-1 monomers, indicating mitochondrial membrane potential dissipation. Merged images indicate co-localization of JC-1 aggregates and monomers. (E) The effect of melatonin and Sirt3 siRNA pretreatment on cell viability. All results are presented as means ± SD of at least three independent experiments. $^{**}p < 0.01$. Ns, not significant.

**Figure 5.** Melatonin increases mitochondrial $O_2\bullet^-$ scavenging by stimulating Sirt3-mediated SOD2 deacetylation. Cells were transfected with Sirt3 siRNA. At 24-h post-transfection, cells were pretreated with melatonin (40 μM) for 2 h and then treated with or without 2 mM fluoride for an additional 12 h. The effect of melatonin and Sirt3 siRNA pretreatment on SOD2 expression (A) and its activity (B). SOD2-deficient L-02 cells were incubated with or without melatonin for 2 h followed by fluoride. (C) Protein expression of Nox4 was detected. (D) SOD2 was immunoprecipitated using Sirt3 antibody. (E) Acetylated-SOD2 (Ac-SOD2) was immunoprecipitated using SOD2 antibody. (F) Ac-SOD2 was immunoprecipitated in Sirt3-deficient L-02 cells. All results are representative of three independent experiments. $^{**}P < 0.01$. Ns, not significant.

**Figure 6.** Melatonin regulates the expression of SOD2 through the interaction of Sirt3 with FoxO3a in mitochondria. Cells were pretreated with melatonin (40 μM) for 2 h and then treated with or without fluoride of 2 mM for an additional 12 h. (A) Mitochondria were isolated after treatment and subjected to western blot analysis

for FoxO3a. (B) FoxO3a was immunoprecipitated using a Sirt3 antibody. Sirt3-deficient L-02 cells were preincubated with or without 40 μM melatonin for 2 h and then treated with or without fluoride (2 mM) for an additional 12 h. (C) FoxO3a acetylation at lysine-100 residue. (D) Cell lysates were harvested for dual luciferase report assays. (E) ChIP analysis was used to examine the binding of FoxO3a to the SOD2 promoter in L-02 cells treated with melatonin. Data are expressed as mean ± SD of three independent experiments. $^{*}P<0.05$, $^{**}P<0.01$ versus the control group.

**Figure 7.** ERRα is required for PGC-1α induced Sirt3 expression. Cells were transfected with PGC-1α siRNA. At 24-h post-transfection, cells were pretreated with melatonin (40 μM) for 2 h and then treated with or without fluoride of 2 mM for an additional 12 h. (A) The expressions of PGC-1α and Sirt3 were measured by western blot. (B) PGC-1α overexpression increased Sirt3 expression and cotransfection of PGC-1α and ERRα could increase more expression of Sirt3. (C) Relative levels of Sirt3 mRNA in response to overexpressed ERRα and fluoride. (D) Overexpression of ERRα followed by melatonin treatment could increase more Sirt3 mRNA levels. ERRα-deficient L-02 cells were preincubated with or without 40 μM melatonin for 2 h and then treated with or without fluoride (2 mM) for an additional 12 h. (E) Relative level of Sirt3 mRNA. All results are presented as means ± SD of at least three independent experiments. $^{*}p < 0.05$, $^{**}p < 0.01$. Ns, not significant.

**Figure 8.** The stimulatory effect of melatonin on the Sirt3 is mediated by the ERR

binding element located between –497 bp and –490 bp upstream of the Sirt3 transcription start site. (A) Cells were transfected with Sirt3 promoter reporter constructs. After transfection, cells were pretreated with melatonin for 2 h and then treated with or without fluoride for an additional 12 h. Left-hand side shows the schematic representation of the Sirt3 promoter reporter constructs. Right-hand side shows the activities of these promoters. (B) The nucleotide sequence from human Sirt3 gene promoter was aligned with corresponding sequences from different species, including mouse and chimpanzee. Evolutionarily conserved elements are indicated in large, bold. (C) Relative levels of WT and MUT Sirt3 promoter activity in response to various treatment. Cell lysates were harvested for dual luciferase reporter assays. (D) *In vitro* binding of ERRα and Sirt3 promoter was examined by EMSA assay using cell lysates from L-02 cells. Left: A preliminary experiment was performed to test the binding of ERRα and WT/MUT probe. Middle: The shift band that comprised protein and probe was regulated by fluoride and melatonin as expected. Right: ERRα antibody was used for supershift. (E) *In vivo* binding of ERRα and Sirt3 promoter was examined by ChIP assay. Fold-enhancement was determined by normalizing threshold cycle values of ERRα ChIP against IgG ChIP. Data are presented as the mean ± SD of three independent experiments. $^{*}P < 0.05$, $^{**}P < 0.01$. Abbreviations: WT, wild type; MUT, mutant.

**Figure 9.** Melatonin activates PGC-1α via activation of PI3K/AKT signaling pathways. (A) Dual luciferase reporter assay results of the cell signaling pathway profiling systems. L-02 cells were transfected with reporter plasmids, as indicated

in Supplemental Table 8, followed by treatment with 40 μM Mel. (B) Relative levels of phosphorylated-AKT and PGC-1α in L-02 cells pretreated with LY294002 (PI3K inhibitor) for 4 h, followed by incubation with 40 μM Mel. (C) Relative levels of Sirt3 promoter activity. Data are presented as the mean ± SD of three independent experiments. $^{**}P < 0.01$.

**Figure 10.** Melatonin upregulates PGC-1α via activation of MT1. Cells were preincubated with Luzindole (10 μM) or MT1 siRNA as described in the Materials and Methods section. (A) The expressions of p-AKT, AKT, and PGC-1α were measured by western blot. (B) Sirt3 promoter activity. Data are presented as the mean ± SD of three independent experiments. $^{*}P < 0.05$, $^{**}P < 0.01$.

**Figure 11.** Melatonin inhibits fluoride-induced JNK1/2 activation in mice liver and L-02 cells. (A) The representative western blot for Bax, Bcl-2, and phosphorylated-JNK1/2 in mice liver. (B) Caspase-3 activity in mice liver. L-02 cells pretreated with SP600125 (10 μM) for 2h, followed by incubation with melatonin or fluoride as indicated. (C) Immunoblot analysis of phosphorylated-JNK1/2 and JNK1/2 in. (D) Caspase-3 activity was detected. (E) The apoptosis rate was determined by flow cytometry. Data are mean ± SD; n = 6–8 or 3 different cultures. $^{*}P < 0.05$, $^{**}P < 0.01$.

**Highlights**

Melatonin reduces sodium fluoride (NaF)-induced mitochondrial superoxide level.

Inhibition of mitochondrial superoxide reduces NaF-induced Nox4 upregulation.

Melatonin mitigates NaF-induced hepatotoxicity by upregulating Sirt3.

Melatonin upregulates Sirt3 expression via activation of PI3K/AKT-PGC-1α pathway.

Melatonin attenuates NaF-induced JNK1/2 activation.